Gain-scheduling Control of CMG Based on Parameter-dependent Lyapunov Function

M2017SC002 Shin INAGAKI
Supervisor : Isao TAKAMI

Abstract

The control moment gyroscope is applied to the attitude control of spacecraft. It has nonlinear characteristics including the trigonometric functions of angle of gimbal. In this research, the nonlinear equation of the system is transformed to a linear one. A linear control theory is applied. Trigonometric functions of angle are approximated by second-order polynomials which have sufficient accuracy. Then, the dynamic equation is represented by an equation of those polynomials. The descriptor representation and Linear Fractional Transformation (LFT) are applied. The linear equation of the angle is obtained. A parameter-dependent Lyapunov function is introduced. LMI conditions are derived to guarantee the stability of the system. A gain scheduling controller is designed using the condition in which the angle of the gimbal is used as a scheduling parameter. The gain scheduling controller can set feedback gains according to the attitude variation, and the control performance is improved. The integral function is added to the controller to suppress the effect of disturbances like frictions. The effectiveness of the proposed controller is illustrated by simulations and experiments.

1 Introduction

A Control Moment Gyroscope (CMG) mounted in satellites and spacecraft generates the gyro torque by tilting the axis of rotor. The CMG can deliver instantly large angular momentum stored in the wheel to the satellite. A reaction wheel (RW) is used as a driving torque generator, but the CMG can generate lager torque than it. The CMG is used as an attitude control device for large scale a spacecraft, for example Skylab, space station Mir and International Space Station (ISS). The CMG in this paper is composed of four rigid bodies, a rotor and three gimbals. Two driving motors are mounted on a rotor (Rotor 1) and a gimbal (Gimbal 2). The driving motor is not mounted on 2 other gimbals (Gimbal 3 and Gimbal 4). The gyro torque generated by Rotor 1 and Gimbal 2 drives Gimbal 3 and Gimbal 4. This is an underactuated system which drives 4 bodied by 2 actuators. The dynamic characteristic of CMG is presented as a nonlinear equation that includes trigonometric functions. Linear approximation is performed on this system, method for designing a linear robust control system is proposed [1]. In [2],[3], methods are proposed to design the gain scheduled control system. However, in [2],[3], the angular velocity of the disk is always designed as a constant angular velocity. In this research, in edition to the gain scheduling control, the robustness of the angular velocity of the disk is guaranteed. Trigonometric functions of gimbal's angle are approximated by second-order polynomials to improve accuracy corresponding to the operating range of CMG. The descriptor representation and linear fractional transformation (LFT) are applied. Also, a linear equation is derived. This equation is affine about the angle of Gimbal and the angular velocity of Rotor that are varying parameters. A parameter-dependent Lyapunov function is defined. The LMI conditions that guarantee stability of the system is derived. The gain scheduled controller is designed depending on the parameter-dependent Lyapunov function. The feedback gain is set according to the attitude of CMG. Also, the control performance is improved. The extended system with an integral of control error added is defined. The controller based on the expanded system is designed to follow the reference, even if there exists a disturbance such as friction. The effectiveness of the proposed method is illustrated by simulations and experiments.

2 Modeling

In this section, the mathematical model of CMG is derived. The schematic diagram of CMG is shown in Figure. 1.

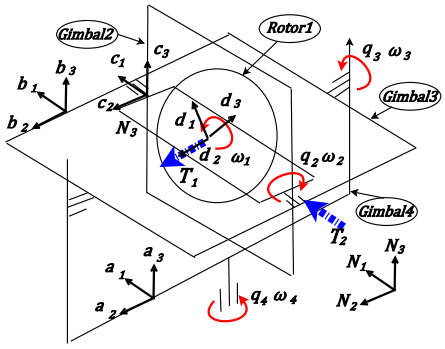

Figure 1 The mathematical model of CMG

The CMG is composed of 4 rotating bodies, Rotor 1, Gimbal 2, Gimbal 3 and Gimbal 4. Two motors are mounted on Rotor 1 and Gimbal2. They generate rotating torques, T_1 and T_2 which drives Rotor and Gimbal 2, directly. The variable q_1 represents the relative angle of Rotor 1 from Gimbal 2. Its velocity is represented by ω_2. The variable q_2 represents the relative angle of Gimbal 2 from Gimbal 3. Its velocity is represented by ω_3. The variable q_3 represents the relative angle of Gimbal 3 from Gimbal 4. Its velocity is represented by ω_4. Similarly, the angular of Gimbal 4 and the angular velocity of Gimbal 4 are q_4 and ω_4, respectively. In this research, it is assumed that the center of gravity of Rotor 1, Gimbal 2, Gimbal 3 and Gimbal 4 are the center of Rotor 1. The influence of gravity is ignored and only the rotational motion is taken account. Rotor 1, Gimbal 2, Gimbal 3 and Gimbal 4 are fixed coordinate systems a_i, b_i, c_i and $d_i (i = 1, 2, 3)$, respectively. The Gimbal 4 rotates around axis a_3. The Gimbal 3 rotates around the axis b_2. Gimbal 2 rotates around the axis c_2. Rotor 1 rotates around the axis d_2. I_v, J_v and K_v are defined as the inertia moment of around axis $1, 2, 3$ of each rigid bodies $v = A, B, C$ and D.

2.1 Derivation of Motion Equation

In this subsection, motion equations of CMG are derived. The trigonometric functions exist in the obtained equations of motion. The trigonometric function is approximated by the second-order polynomials to improve the precision. It can correspond to the large range of gimbal's operating point. Let scheduling parameters be q_2 and q_3 that vary largely by the attitude control of CMG. The equations of motion for q_1, q_2, q_3, q_4 are derived by Lagrange equation $\mathcal{L}$. There are written as follows,

$$f_1(q_2, q_3, \omega_2, \omega_3, \omega_4, \dot{\omega}_1, \dot{\omega}_3, \dot{\omega}_4) = T_1, \quad (1)$$
$$f_2(q_2, q_3, \omega_1, \omega_3, \dot{\omega}_1, \dot{\omega}_2) = T_2, \quad (2)$$
$$f_3(q_2, q_3, \omega_1, \omega_2, \omega_3, \omega_4, \dot{\omega}_1, \dot{\omega}_3, \dot{\omega}_4) = 0, \quad (3)$$
$$f_4(q_2, q_3, \omega_1, \omega_2, \omega_3, \omega_4, \dot{\omega}_1, \dot{\omega}_2, \dot{\omega}_3\dot{\omega}_4) = 0. \quad (4)$$

2.2 Derivation of State Space Representation

In this subsection, a state space representation is derived by Eq.(1)-(4). Here, the range of the Gimbal 2 and the Gimbal 3 are supposed as $-\frac{\pi}{4.5} \leq q_2 \leq \frac{\pi}{4.5}$ and $-\frac{\pi}{4.5} \leq q_3 \leq \frac{\pi}{4.5}$, respectively. Usually, Taylor expansion is given as a primary approximation that $\sin(x) \approx x, \cos(x) \approx 1$, then $x = \frac{\pi}{4.5}$ in $\cos(x)$, the difference between the approximation and the true value is 0.234. This can not to be ignored. Here, a second-order approximation is taken as $\sin(x) \approx x, \cos(x) \approx 1 - \frac{x^2}{2}$. An approximation accuracy of the equation is shown in Figure. 2-3.

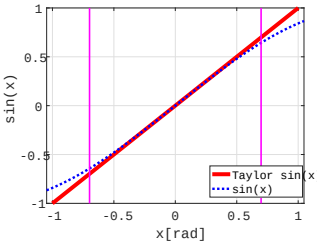

Figure 2 $\sin(x)$

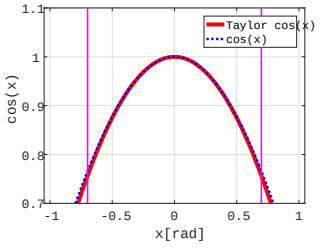

Figure 3 $\cos(x)$

The red solid line shows approximated values of sine and cosine. The blue dotted lines show the true value of sine and cosine respectively. Then $x = \frac{\pi}{4.5}$ in $\cos(x)$, the difference between the second-order approximation and the true value is 0.0097. The second-order approximation is adopted because the accuracy of second-order approximation is better than the first-order approximation. The approximation is substituted in Eq.(1)-(4). Let a state variable vector be $x(t) = [q_3\ q_4\ \omega_2\ \omega_3\ \omega_4]^{\mathrm{T}}$. The state space representation is written as follows,

$$\dot{x}(t) = \begin{bmatrix} 0 & 0 & 0 & 1 & 0 \\ 0 & 0 & 0 & 0 & 1 \\ 0 & 0 & & & \\ 0 & 0 & & -F^{-1}G & \\ 0 & 0 & & & \end{bmatrix} x(t) + \begin{bmatrix} 0 & 0 \\ 0 & 0 \\ & \\ & F^{-1}H \\ & \end{bmatrix} u(t), \quad (5)$$

$$F = \begin{bmatrix} a_1 & 0 & a_2 \\ 0 & a_3 & a_4 \\ -a_1 & a_4 & a_5 \end{bmatrix}, \ G = \begin{bmatrix} 0 & b_1 & b_2 \\ b_3 & 0 & -b_3 \\ -b_2 & b_3 & b_4 \end{bmatrix}$$

$$H = \begin{bmatrix} 0 & 1 \\ c_1 & 0 \\ c_2 & 0 \end{bmatrix}$$

$$a_1 = J_a,\ a_2 = -J_a q_3,\ a_3 = J_B + J_C + J_b q_2^2,$$

$$a_4 = J_b(q_2 - \frac{2}{3}q_2^3)(1 - \frac{q_3^2}{2}),$$

$$a_5 = K_A + I_D + (K_B + K_C)(1 - q_3^2) + I_C q_3^2 + J_b q_2^2(1 - q_3^2),$$

$$b_1 = J_D \omega_1 q_2, b_2 = -J_D \omega_1 (1 - \frac{q_2^2}{2})(1 - \frac{q_3^2}{2}),$$

$$b_3 = -J_D \omega_1 q_2 q_3, b_4 = I_C q_3^2, c_1 = -1 + \frac{q_2^2}{2}, c_2 = -q_2(1 - \frac{q_3^2}{2}),$$

$$J_a = I_C + I_D, J_b = J_C - K_C - K_D.$$

If a parameter ω_1 and q_2 are included in the state variable, the state variable becomes uncontrollable. Therefore, the parameter ω_1 and q_2 can not included in the state variable. In this study, to make the output follow the reference without error, the system is expanded. Let the reference of q_3 and q_4 be q_3^{ref} and q_4^{ref} respectively. Then, a state equation is written as follows,

$$\dot{x}_e(t) = A_e x_e(t) + B_e u(t), \quad (6)$$

$$A_e = \begin{bmatrix} 0 & 0 & -1 & 0 & 0 & 0 & 0 \\ 0 & 0 & 0 & -1 & 0 & 0 & 0 \\ 0 & 0 & 0 & 0 & 0 & 1 & 0 \\ 0 & 0 & 0 & 0 & 0 & 0 & 1 \\ 0 & 0 & 0 & 0 & & & \\ 0 & 0 & 0 & 0 & & -F^{-1}G & \\ 0 & 0 & 0 & 0 & & & \end{bmatrix}, \ B_e = \begin{bmatrix} 0 & 0 \\ 0 & 0 \\ 0 & 0 \\ 0 & 0 \\ & \\ & F^{-1}H \\ & \end{bmatrix}.$$

3 Control Design

3.1 Descriptor Representation

In this section, the state equation is linearized by descriptor representation. The matrices A_e and B_e contain time variable parameters q_2 and q_3. The time variable parameters must be aggregated into one coefficient matrix. Let the descriptor vector be $x_d = [x_e(t)^{\mathrm{T}}\ \omega_2\ \omega_3\ \omega_4\ T_1]^{\mathrm{T}}$, the descripter representation is written as follows,

$$E_d \dot{x}_d(t) = A_d x_d(t) + B_d u_d(t), \quad (7)$$

$$A_d = \begin{bmatrix} O_{2\times2} & -I_2 & O_{2\times3} & O_{2\times3} & O_{2\times1} \\ O_{5\times2} & O_{5\times2} & M & N & O_{5\times1} \\ O_{3\times2} & O_{3\times2} & -G & -F & L \\ O_{1\times2} & O_{1\times2} & O_{1\times3} & O_{1\times3} & -1 \end{bmatrix},$$

$$M = \begin{bmatrix} O_{2\times1} & I_2 \\ O_{3\times1} & O_{3\times2} \end{bmatrix}, \ N = \begin{bmatrix} O_{2\times3} \\ I_3 \end{bmatrix}, \ L = \begin{bmatrix} 0 \\ c_1 \\ c_2 \end{bmatrix}$$

$$E_d = \begin{bmatrix} I_7 & O_{7\times4} \\ O_{4\times7} & O_{4\times4} \end{bmatrix}, \ B_d = \begin{bmatrix} O_{6\times2} \\ 0 & 1 \\ 0 & 0 \\ 0 & 0 \\ 1 & 0 \end{bmatrix}.$$

3.2 linearized by Linear Fractional Transformation(LFT)

In this section, the state equation is linearized by Linear Fractional Transformation (LFT). However, the matrix A_d in (7) contained cubic terms. Also, a computable LMI condition can not be derived when parameter-dependent Lyapunov Function is used. In this research, the matrix A_d is equivalently transformed to an affine form not including the square term of scheduling parameter. A method that the scheduling parameter is taken out by linear fraction transformation (LFT) is applied to perform the conversion. This equation is written as follows,

$$\widetilde{A}_d(t) = A_n + B_\delta(I - \Delta D_\delta)^{-1}\Delta C_\delta. \tag{8}$$

Then, Equation (8) is rewritten as follows,

$$\begin{cases} E_d\dot{x}_d = A_n x_d + B_\delta w_\delta + B_d u \\ z_\delta = C_\delta x_d + D_\delta w_\delta \\ w_\delta = \Delta z_\delta \end{cases}, \tag{9}$$

where

$$\Delta = \mathrm{diag}([q_2, \ldots, q_2, q_3, \ldots, q_3]).$$

A new descriptor variable is given as $\widetilde{x} = \begin{bmatrix} x_d^{\mathrm{T}} & z_d^{\mathrm{T}} \end{bmatrix}^{\mathrm{T}}$. The system can be transformed to a computable LMI condition. The equation using the descripter representation with LFT is written as follows,

$$\widetilde{E}_d\dot{\widetilde{x}}_d(t) = \widetilde{A}_d\widetilde{x}_d(t) + \widetilde{B}_d u(t), \tag{10}$$

$$\begin{aligned} \widetilde{A}_d &= A_0 + q_2A_1 + q_3A_2 + \omega_1A_3 \\ &= \begin{bmatrix} A_n & B_\delta\Delta \\ C_\delta & -I + D_\delta\Delta \end{bmatrix}, \\ \tilde{E}_d &= \begin{bmatrix} E_d & 0 \\ 0 & 0 \end{bmatrix}, \quad \tilde{B}_d = \begin{bmatrix} B_d \\ 0 \end{bmatrix}. \end{aligned} \tag{11}$$

A parameter box whose vertices are the upper and lower bounds of the variation parameter is given by

$$\Theta = \{\theta = [\theta_1, \theta_2, \theta_3, \theta_4, \theta_5]^{\mathrm{T}} : \theta_i \in \{\underline{\theta_i}, \overline{\theta}_i\}\} \ (i = 1, \ldots, 5) \tag{12}$$

$$\theta_1 = q_2,\ \theta_2 = q_3,\ \theta_3 = \omega_1,\ \theta_4 = \omega_2,\ \theta_5 = \omega_3.$$

4 Gain Scheduling Controller [4]

In this section, the gain scheduling controller based on the Lyapunov function for the closed loop system is designed that the state feedback control law $u = K(\theta)x$ is given to the descriptor system (10). In this research, a gain scheduling controller is designed based on the optimum regulator which minimizes the following evaluation function

$$J = \int_0^\infty (\widetilde{x}_d(t)^{\mathrm{T}} Q \widetilde{x}_d(t) + u(t)^{\mathrm{T}} R u(t))dt, \tag{13}$$

where $Q \geq 0, R > 0$.

The Lyapunov matrix $X_d(\theta)$ and the transformation matrix $Y_d(\theta)$ are given as follows,

$$X_d(\theta) = X_{d0} + \theta_1 X_{d1} + \theta_2 X_{d2}, \tag{14}$$

$$Y_d(\theta) = Y_{d0} + \theta_1 Y_{d1} + \theta_2 Y_{d2}. \tag{15}$$

The matrix X_{di} and Y_{di} have the following structures,

$$X_{di} = \begin{bmatrix} X_i & 0 & 0 \\ X_{21,i} & X_{22,i} & X_{23,i} \\ X_{31,i} & X_{32,i} & X_{33,i} \end{bmatrix}, \tag{16}$$

$$Y_{di} = \begin{bmatrix} Y_i & 0 & 0 \end{bmatrix} (i = 0, 1, 2). \tag{17}$$

The following parameter box's vertices $\Theta_j (j = 1, \cdots, 32)$ are defined as the vertex matrices. These box's vertex are written as follows,

$$\Theta_1 = (\underline{\theta_1}, \underline{\theta_2}, \underline{\theta_3}, \underline{\theta_4}, \underline{\theta_5}), \Theta_2 = (\overline{\theta_1}, \underline{\theta_2}, \underline{\theta_3}, \underline{\theta_4}, \underline{\theta_5}),$$
$$\ldots \Theta_{15} = (\underline{\theta_1}, \overline{\theta_2}, \overline{\theta_3}, \overline{\theta_4}, \overline{\theta_5}), \Theta_{32} = (\overline{\theta_1}, \overline{\theta_2}, \overline{\theta_3}, \overline{\theta_4\theta_5}).$$

Since $\dot{\widetilde{X}}_d(\theta)$ is

$$\dot{\widetilde{X}}_d(\theta) = \dot{\theta}_1 X_{d1} + \dot{\theta}_2 X_{d2}, \tag{18}$$

$$\widetilde{X}_d(\dot{\theta}) = X_{d0} + \dot{\theta}_1 \dot{X}_{d1} + \dot{\theta}_2 X_{d2}. \tag{19}$$

Eq(18)-(19) are written as follows,

$$\dot{\widetilde{X}}_d(\theta) = \widetilde{X}_d(\dot{\theta}) - \dot{X}_{d0} \tag{20}$$

$$E_d\dot{\widetilde{X}}_d = \begin{bmatrix} X(\dot{\theta}) - X_0 & 0 & 0 \\ 0 & 0 & 0 \\ 0 & 0 & 0 \end{bmatrix}, \tag{21}$$

where

$$X(\dot{\theta}) = X_0 + \dot{\theta}_1 X_1 + \dot{\theta}_2 X_2. \tag{22}$$

Let set $C_d = [W_x\ 0\ 0], W_x = [Q^{\frac{1}{2}}\ 0]^{\mathrm{T}}$ and $D_d = [0\ R^{\frac{1}{2}}]$. The LMI condition for the gain scheduling control is written as follows,

$$minimize : \gamma \tag{23}$$

$$subject\ to : X(\Theta_j) \succ 0 \tag{24}$$

$$\begin{bmatrix} \mathrm{He}[\widetilde{A}_d(\Theta_j)X_d(\Theta_j) + B_dY_d(\Theta_j)] - S_d(\Theta_i) & X_d(\Theta_j)^{\mathrm{T}}C_d^{\mathrm{T}} + Y_d(\Theta_j)^{\mathrm{T}}D_d^{\mathrm{T}} \\ C_dX_d(\Theta_j) + D_dY_d(\Theta_j) & -I \end{bmatrix} \prec 0$$

$$(j = 1,\ \ldots,\ 32) \tag{25}$$

$$\begin{bmatrix} W & I \\ I & X(\Theta_k) \end{bmatrix} \succ 0 \quad (k = 1,\ \ldots,\ 8) \tag{26}$$

$$\mathrm{trace}(W) < \gamma, \tag{27}$$

where $S_d(\dot{\Theta}_j) = \mathrm{diag}[(X(\dot{\Theta}_j) - X_0, 0, 0)]$. However, Eq. (25) contains $A_d(\Theta_j)X_d(\Theta_j)$. Eq. (25) does not become multi-affine because there is a squared term. The $A_d(\Theta_j)X_d(\Theta_j)$ is given a constraints to be multi-affine. The $X(\theta)$ and the $Y(\theta)$ are obtained by LMI condition from there equations. The GS state feedback $u(t)$ based on the parameter dependent Lyapunov function in the framework of the descriptor representation is given as follows,

$$\begin{aligned} u &= K_d\widetilde{x}_d = Y_d(\theta)X_d(\theta)^{-1}\widetilde{x}_d(t) \\ &= [Y(\theta)\ 0\ 0] \begin{bmatrix} X(\theta) & 0 & 0 \\ X_{21}(\theta) & X_{22}(\theta) & X_{23}(\theta) \\ X_{31}(\theta) & X_{32}(\theta) & X_{33}(\theta) \end{bmatrix}^{-1} \widetilde{x}_d(t) \\ &= Y(\theta)X(\theta)^{-1}x_e(t), \end{aligned} \tag{28}$$

where

$$X(\theta) = X_0 + \theta_1 X_1 + \theta_2 X_2, \tag{29}$$

$$Y(\theta) = Y_0 + \theta_1 Y_1 + \theta_2 Y_2. \tag{30}$$

5 Experiment

In this section, the effectiveness and validity of the designed controller are illustrated by the simulation and experiment results. Simulation results and experiment results are compared by the Gain Scheduling controller and robust LQ controller of fixed gain. Let x and ω_1 be $x_0 = [0,0,0,0,0,0], \omega_1 = 43.9823$[rad]. The upper bound and lower bound of the fluctuation parameter $\omega_1, q_2, \omega_2, q_3, \omega_3$ are determined as follows,

$$\omega_1 \in [20.94,\ 62.83][\text{rad}], \tag{31}$$

$$q_2 \in [-\frac{\pi}{4.5},\ \frac{\pi}{4.5}][\text{rad}],\ \omega_2 \in [-1,\ 1][\text{rad/sec}], \tag{32}$$

$$q_3 \in [-\frac{\pi}{4.5},\ \frac{\pi}{4.5}][\text{rad}],\ \omega_3 \in [-1,\ 1][\text{rad/sec}], \tag{33}$$

The weight matrix Q and R was set as follows,

$$Q = diag[(1\ 0.5\ 0.5\ 0.5\ 0.5\ 0.1\ 0.1)].\ R = diag[(1\ 1)]. \tag{34}$$

The upper bound values of gain scheduling control and the fixed gain robust LQ control are shown in the Table 1.

Table 1 Upperbound

	Nominal	GS	Robust LQ
Upper bound	$\gamma = 1.1284$	$\gamma = 2.0083$	$\gamma = 2.6853$

Eq. (28) of K_d is written as follows,

$$Y(\theta)X(\theta)^{-1} = K_d(\theta) = \begin{bmatrix} K_{11} & K_{12} & K_{13} & K_{14} & K_{15} & K_{16} & K_{17} \\ K_{21} & K_{22} & K_{23} & K_{24} & K_{25} & K_{26} & K_{27} \end{bmatrix} \tag{35}$$

The feedback gain K_{14} and K_{24} are shown in Figure 4 and 5 as a function of scheduling parameter q_2 and q_3.

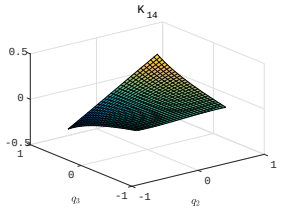

Figure 4 K_{14}

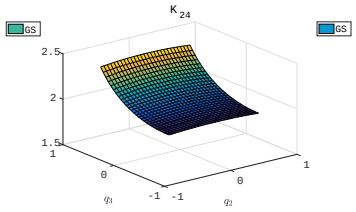

Figure 5 K_{24}

From the Figure 4-5 that the gain is adjusted by the gain scheduling control. The angle of Gimbal 3 and angle Gimbal 4 of experiment results are shown in Figure 6-7. The solid line shows the experimental result of GS. The dashed line shows the experimental result of robust LQ. The dotted line shows the command, respectively. As can seen in Figure6, the GS has better performance than robust LQ. Torque of Motor 1 T_1 and torque of Motor 2 T_2 are shown Figure 8-9, respectively. The input constraint range of T_1 and T_2 are $-0.6 \leq T_1 \leq 0.6, -2.4 \leq T_2 \leq 2.4$, respectively.

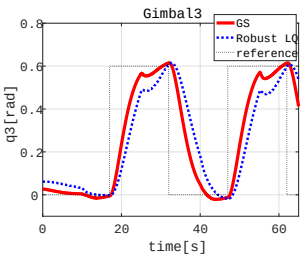

Figure 6 Gimbal3

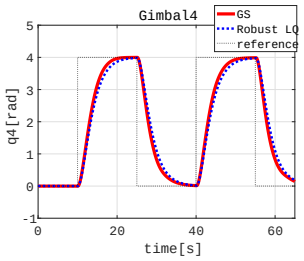

Figure 7 Gimbal4

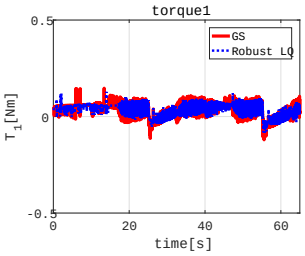

Figure 8 T_1

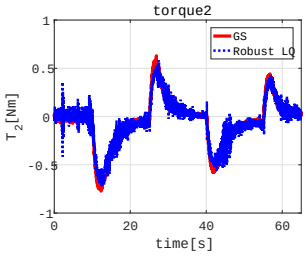

Figure 9 T_2

6 Conclusion

In this research, the dynamic characteristics of Control Moment Gyroscope (CMG) is represented by mathematical model. It is linearized by performing second order approximation of Taylor expansion, descriptor representation and Linear Fractional Transformation (LFT). From the linearized system, we designed the gain scheduling controller of the linear matrix inequality (LMI). Moreover, by introducing an integrator, it can follow the reference without error. The usefulness of the GS control is shown by the experimented results computing with the robust LQ controller. The robustness of the angular velocity of the Rotor 1 was guaranteed.

References

[1] Toru Inaba Chinatsu Murai Gan Chen and Isao Takami: Robust Control of Control Moment Gyroscope with Friction Disturbance -Using Polytopic Representation- 2015 7th International Conference on Information Technology and Electrical Engineering, pp.559-564, 2015.

[2] Hossam S. Abbas, Ahsan Ali, Seyed M. Hashemi and Herbert Werner: LPV Gain-Scheduled Control of a Control Moment Gyroscope, 2013 American Control Conference(ACC), pp. 6857-6862, 2013.

[3] Toru INABA and Isao TAKAMI: Gain Scheduling Control of Control Moment Gyroscope, Graduate Program of Mechatronics Graduate School of Science and Engineering Nanzan University, 2016.

[4] G. Chen: System analysis using redundancy of descriptor representation. Computer Aided Control System Design, 2004 IEEE International Symposiump, pp.231-236, 2004.